

J-Integral and Cyclic Plasticity Approach to Fatigue and Fracture of Asphaltic Mixtures

A. A. ABDULSHAFI and KAMRAN MAJIDZADEH

ABSTRACT

A nationwide survey of pavement performance indicated that fatigue is the most important distress problem in U.S. primary pavements. The classical approaches to investigating fatigue problems are classified as phenomenological and mechanistic. The phenomenological approach is based on developing a distress function using laboratory simulation of third-point beam loading, beam on elastic foundation, discs, and so forth; its main drawback is that most of the fatigue life is exhausted through cyclic plasticity, and crack initiation, propagation, and ultimate failure, with the associated stress and strain redistributions, are not accounted for. The mechanistic approach is based on the laws of linear elastic fracture mechanics (LEFM) to model laboratory-simulated crack initiation, propagation, and unstable failure; its main shortcoming is that failure is assumed to be by brittle fracture and the initiation phase is not modeled because it is assumed that a crack size of " c_0 " initially exists. Moreover, the stress intensity factor requires rather specialized computational techniques like finite elements. In this paper, a cyclic plasticity fatigue model is developed through laboratory-controlled stroke fatigue testing of unnotched disc samples of asphaltic mixes. This model is statistically matched with controlled stroke fatigue testing of notched discs under the same stroke range loading condition. Another model is developed for fatigue crack propagation using the elasto-plastic fracture mechanics (EPPM) approach. The EPPM fracture criterion is the path-independent contour J-integral. Within the development of the propagation model, a method for J-integral testing of asphaltic mixtures has been established. An example is presented and worked out to illustrate how this new approach can be used in modeling fatigue life.

A nationwide survey of pavement performance (1) indicated that fatigue of primary pavements is generally the most important distress type. Fatigue is defined as "the phenomenon of fracture under repeated or fluctuating stress having a maximum value much less than the tensile strength of the material" (2). In connection with this definition, a failure criterion has to be defined. Failure is a complex process that is based on the damage accumulation concept. An introduction to the mechanisms by which damage progresses in the continuum under load applications is instructive in casting light on the failure manifestations.

Damage can be defined as a structure-sensitive property that is imparted to the material through the influence of defects (microscopic or macroscopic cracks, voids, dislocations, and so forth) that are naturally or artificially introduced, thereby rendering the material inhomogeneous (3). The progression of damage under load applications is due to internal irregularities or defects that grow gradually to a certain critical size; thereafter, growth is unstable. In engineering materials, damage has been categorized by two different conditions: ductile (plastic flow) or brittle (elastic fracture). This implies that fatigue is not, in itself, a single physical phenomenon but rather a condition brought about by several different processes that may lead to the disintegration of a body by the action of mechanical forces (4). Damage may therefore progress within a material under the different mechanisms of fracture and flow, depending on critical values of stresses, strains, and environmental and temperature conditions. A material may have more

than one characteristic parameter to be evaluated when different damage mechanisms operate at critical levels.

It can be postulated that cracks (not voids that are considered probabilistic crack initiators) and plastic deformation (which may be accompanied by viscous flow) are valid material failure criteria. Observations of the type of failure occurring within a continuum can reveal which condition dominates during the damage process. However, in real-life materials, the state responsible for damage reverses randomly, making fracture and plastic deformation equally probable. The distribution and progression of damage are random processes that are spatial, time dependent, and temporal. Whether or not a continuum exhibits fracture or inelastic flow depends on many factors, including the normal stresses, the tensile or shear stress required to cause fracture, the shear stresses, the shear stress required for inelastic flow, and moisture and temperature conditions.

CLASSICAL APPROACHES TO FATIGUE PROBLEMS

Approaches to the fatigue problem can be classified as phenomenological or mechanistic. In the first approach, laboratory testing of a beam or disc under controlled load (stress) or controlled stroke (strain) loading mode is used to develop stress or strain versus number of cycles to failure (S-N) curves. Due to the scatter of results, a regression analysis is usually employed to fit the obtained

data and arrive at a mathematical expression (distress function) such as that of Pell's equation (5):

$$N_f = c(1/\sigma \text{ or } \epsilon)^m \quad (1)$$

where

- N_f = number of load applications to failure;
- ϵ = amplitude of applied tensile strain in controlled strain mode;
- σ = amplitude of applied stress in controlled stress mode; and
- c, m = factors that depend on the material composition, mix properties, and loading mode.

Research has indicated (6) that controlled strain mode is appropriate for thin (2 in. or less) pavements and controlled stress mode is appropriate for thick stiff pavements (greater than 6 in.). Between these two ranges in thickness, some form of loading intermediate to both controlled strain and stress is appropriate. Investigations in the past 20 years have been concerned with effects of factors such as using trapezoidal-shaped cantilever beams (7-9), compound loadings (10), frequency (11), and rest periods (12) on the distress function. In short, it has been noted that although this approach gained universal acceptance, its limitation is that it cannot account for crack initiation and propagation and the subsequent redistribution of stresses within the layered system (13).

Mechanistic approaches using the application of fracture mechanics are based on nominal or local stress-strain analysis. It has been speculated that the major deficiencies in inaccurate prediction of fatigue life based on nominal stress analysis could be overcome if local stress-strain in the immediate vicinity of a stress raiser were considered instead.

The nominal stress-strain mechanistic approach developed at Ohio State University is credited to Majidzadeh et al. (14). This approach is based on the postulate that fatigue life can be described by the process of crack initiation, propagation, and ultimate fracture. These three damage processes include material parameters that can characterize fatigue and fracture and that can be related as

$$N_f = \phi(c_o, A, n, K, KIC) \quad (2)$$

such that

$$dc/dN = \sum A_i K^{n_i} \quad (3)$$

where

- c_o = initial crack length,
- A, n = material constants,
- K = elastic stress intensity factor, and
- KIC = elastic fracture toughness.

A and n are affected by such parameters as load frequency, external boundary conditions, temperature, and statistical distributions of flaws in the materials as well as the dimensions of the models used. Extensions to Majidzadeh's work in applying linear elastic fracture mechanics (LEFM) include research studies on the effects of frequency (5), crack tip plasticity (15), and wave form and compound loading (16) on crack propagation; however, the idea of using LEFM remains the same.

Laboratory experimentation to find the fracture-fatigue function involves testing a beam on an elastic foundation and monitoring crack advance versus the number of load applications. The data thus obtained can be fitted by least squares approximation

procedures of regression analysis to arrive at a best fit. A two-term model fit can take the form:

$$dc/dN = a_1 K_1 + a_2 K_1^2 \quad (4)$$

implying that

$$\int_0^{N_f} dN = \int_{c_o}^{c_f} [dc/(a_1 k_1 + a_2 k_1^2)] \quad (5)$$

Hence,

$$N_f = \int_{c_o}^{c_f} [dc/(a_1 k_1 + a_2 k_1^2)] \quad (6)$$

NEW CONCEPTS IN FATIGUE MODELING OF ASPHALTIC MIXTURES

Introduction

In a laboratory-controlled setting, given a valid constitutive law, it should be possible to predict laboratory sample performance, namely rutting and fatigue in asphaltic mixtures, with reasonable accuracy. Both laboratory and field investigation indicate that the failure of asphaltic mixes for a given set of loading conditions could be due to rutting (permanent deformation), fatigue cracking, or a combination of the two. Whether material parameters are stress or environment dependent, or both, is a subject of controversy.

The authors are inclined to believe that the material will exhibit a range of characteristic behavior within which the material parameters are uncoupled from stress and environmental conditions. Further, examination of sample failures will reveal the states that dominate at the unstable failure conditions. That is where laboratory samples attain their importance as an indicator of field performance.

Following this point leads to another point of controversy--simulation of the fatigue problem. It has been argued that fatigue life determined from small laboratory specimens could be misleading in determining the fatigue life of an actual pavement (14,16); this is because it has been observed that most of the fatigue life of a small, smooth, unnotched specimen will be consumed in initiating a crack and, therefore, the final stages of crack propagation and ultimate failure become indistinguishable within the data scatter (16-18, p.132). The question of whether these are typical of field observations cannot be directly addressed; however, inconsistent correlations of fatigue life predicted from laboratory testing indicate that more research needs to be done.

To better simulate the failure conditions or determine where the importance of fracture toughness lies, fracture conditions must be induced in the small specimens. To promote early crack growth, it is proposed that notched specimens be used. A model could then be developed to make a comparison between notched and unnotched specimens, and another model could be developed for crack growth.

In the analysis of unnotched specimens, cyclic plasticity and energy balance should be the tools by which the analysis is effected. On the other hand, the notched specimens should be investigated within the framework of local stress-strain analysis that will directly introduce the elasto-plastic (or time-dependent) fracture mechanics approach.

Exhaustion of Ductility Model (unnotched samples)

Fatigue life passes through three distinct periods: initiation of a crack, propagation of the crack to a

critical size, and ultimate failure. In each life period, there is a damaging mechanism or mechanisms that exhaust energy and lead to transition to the other phase. Many research studies have been done, especially in metallurgical engineering, postulating theories for the cause or causes of fatigue; however, most of these theories conclude that inhibition of fine slips that grow to a crack that will subsequently propagate and lead to ultimate failure is the cause of fatigue. Morrow (17) explained that, on the microscopic level, the cyclic plastic strain is related to the movement of dislocations, and the cyclic stress is related to the resistance to their motion. According to Morrow, repeated stress without accompanying plastic strain will not cause fatigue damage nor would repeated slip without repeated stress. He also suggested a tentative set of six fatigue fracture properties that are shown to apply well to SAE 4340 steel. These six fatigue properties will be examined to determine their applicability to asphalt fatigue models.

These properties are associated with coefficients that could be obtained from controlled stroke laboratory fatigue experimentation shown in Figure 1 as b , c , and ϵ_f , and from S_f and S . The mathematical representation of the suggested fatigue model is

$$\Delta\epsilon/2 = \sigma_f (2N_f)^b + \epsilon_f' (2N_f)^c \quad (7)$$

The first four coefficients will be defined later, and S_f is the strength limit (associated with endurance limit) and S is the standard deviation of data scatter.

The controlled stroke fatigue coefficients shown in Figure 1 are defined as

- ϵ_f' = fatigue ductility coefficient--the strain intercept of the ductility line at $N = 1$ cycle; it is related to ϵ_f , where ϵ_f = the monotonic fracture ductility;
- σ_f = fatigue strength coefficient--the strain intercept of the strength line at $N = 1$ cycle divided by E ; it is related to σ_f , where σ_f = the monotonic fracture strength;
- b = fatigue strength exponent--the slope of the strength line; and
- c = fatigue ductility exponent--the slope of the ductility line.

The idea of this scheme is to construct the fatigue curve without the need for doing "fatigue testing." This can be done by evaluating the mono-

tonic coefficients (ϵ_f , σ_f , and E) and using the universal slopes b and c . The universal slopes are well established in the metallurgical engineering field; however, their applicability to asphaltic mixtures has not been researched until now.

The scheme of characterizing fatigue through six coefficients is advantageous in that the coefficients relate to other engineering properties of asphaltic mixtures that are routinely determined. The mathematical expressions for this model will be referenced in a later section. This model applies to ductile failures where "cracking life is short" and used with a brittle failure model to predict crack initiation life.

The main criticism of the scheme is that field performance is not simulated by using small laboratory samples that exhaust most of their fatigue life in the crack initiation phase. The model that replicates field conditions should contain crack propagation and ultimate failure matched with the cyclic plasticity model. Matching criteria should be modeled by an expression for the actual number of cycles to initiate a crack. This will be addressed in a subsequent section of this paper.

Fracture Mechanics Considerations

Plastic zones created in the material when it is subjected to alternating low stress levels are mainly due to crack presence. In addition, during each loading cycle the sharp aggregate corners transmit point loading conditions to the asphalt cement with a stress singularity. Hence, even before crack formation, a plastic zone exists at each (sharp aggregate corner-asphalt cement) contact, and energy is dissipated through cyclic plasticity. Once a crack is initiated, then at the tip of the crack, stresses assume an inverse, square root stress (and strain) singularity. Because the material can tolerate stresses up to its yield point, a plastic zone around the crack tip forms and blunts the crack advance. The size of this plastic zone is critical in the analysis of fatigue life. If the formed plastic zone is small compared to the crack size and the geometry of the continuum, linear elastic fracture mechanics (LEFM) is approximating conditions of failure favorably (small scale yielding). On the other hand, if the size of the plastic zone cannot be ignored (several orders of magnitude of the crack size), a nonlinear fracture mechanics approach is more appropriate.

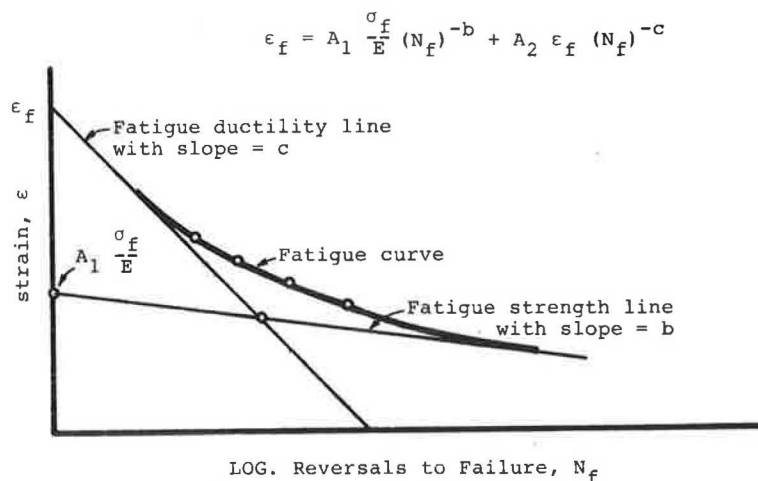


FIGURE 1 Controlled stroke fatigue diagram--fatigue coefficients.

In asphaltic mixtures, cracks usually develop at the bottom of the asphaltic layer due to tensile stresses exceeding a threshold yield stress value. This provides an opening mode fracture, designated as Mode I. Further, the crack propagates vertically but in a zig-zag path, indicating either an aggregate obstruction or a weak contribution of Mode II loading type; however, for all practical purposes, Mode I can be considered dominating.

Hence, in the first case (LEFM), the material is assumed to exhibit brittle fracture (KI dominant region) where the Mode I critical stress intensity factor (K_{IC}) is the material fracture characteristic. In the second case, the material is assumed to exhibit ductile fracture (J-dominant region) where J_{IC} represents the material elasto-plastic fracture characteristics.

Bituminous mixtures can exhibit brittle or ductile fracture, depending on the state of stress at failure, which, in turn, depends on such factors as temperature, loading conditions, hardening or softening induced, and inherent properties. Furthermore, the literature indicates that (19)

$$J_1 = K_1/E'^2 = G_1 = \gamma \delta_t \cdot \sigma_y$$

$$E' = \begin{cases} E \text{ plane stress} \\ E/1 - \nu^2 \text{ plane strain} \end{cases} \quad (8)$$

where

- J₁ = path-independent Mode I contour J-integral,
- K₁ = Mode I elastic stress intensity factor,
- E = uniaxial elastic modulus,
- ν = Poisson's ratio,
- G₁ = strain energy release rate,
- δ_t = crack opening displacement,
- σ_y = yield strength, and
- γ = scalar multiplier.

At the incipient crack conditions, the fracture criterion is

$$K_1 = K_{IC} \text{ and } J_1 = J_{IC} \quad (9)$$

and the relationships given in Equation 8 hold.

In fact, Begley and Landes (19) have used small, fully plastic specimens to determine J_{IC} values. These values were found to be in good agreement with K_{IC} values obtained from large independent elastic specimens that satisfied plane strain fracture toughness requirements.

It is apparent then that J_{IC} is an appropriate material characterization for both elastic and elasto-plastic fracture mechanics approaches. The experimental evaluation of J and J_{IC} can be found elsewhere (20). The basic idea behind the development of a J-integral testing procedure is to interpret the J-integral as the energy release rate (19); then,

$$J = (-1/B) (\partial u / \partial a) |_{\Delta} \quad |_{\Delta} \text{ means } \Delta \text{ is held fixed} \quad (10)$$

where

- B = specimen thickness,
- U = total strain energy,
- a = crack length, and
- Δ = load-point displacement.

For simplicity, elastic unloading is considered only at the fracture point for the monotonic loading, and U can be found as the area under the load-displacement curve. Development of the appropriate fracture mechanics models to describe the fatigue

life of asphaltic mixtures is considered in the next section.

Development of Fatigue Fracture Models

Fatigue Crack Propagation Model (notched sample)

To promote crack propagation, a notch has to be introduced into the sample, together with a fine, sharp-edged crack. Manson (16) has suggested that

$$dc/dN = A \cdot c \quad (11)$$

where

- c = crack length,
- N = number of cycles at crack length c, and
- A = material constant.

The LEFM considers

$$K_1 \Rightarrow \sigma c^{1/2} \dots \quad c \Rightarrow K_1^2 / \sigma^2 \quad (12)$$

The extension of the J-integral to the elastic case gives (from Equation 8)

$$J_1 = K_1^2 / E'$$

Substituting into Equation 12 gives

$$C = JE' / \sigma^2 = J / \sigma \Sigma_E = J / 2U_e \quad (13)$$

where U_e is elastic strain energy and J is J(c,U) where U is the total strain energy.

Substitute Equation 13 into Equation 11 to get

$$dc/dN = A(J/2U_e) \quad (14)$$

Equation 14 represents the crack propagation model. Experimentally (20) (a) a J-c curve will be established, where U_e can also be found and (b) a c-N relationship will be found by performing fatigue tests on notched specimens. This relationship will be differentiated to obtain the (dc/dN) versus N relationship. Now, for certain N, c and dc/dN can be obtained. From (a), J that corresponds to c can be obtained and then the relationship (dc/dN) - J can be established. The slope of this relationship should be A/2U_e.

Crack Initiation Model

Only a theoretical model is discussed in this section because crack initiation will be determined experimentally by monitoring the number of cycles to propagate different size cracks of the disc specimens. The theoretical discussion of the crack initiation models serves as an introduction to a follow-up paper.

From Equation 14,

$$dN = (2U_e/AJ) \cdot dc = dJ / (J \cdot A) \quad (15)$$

Therefore,

$$\int_{N_0}^N dN = \int_{J_0}^J (dJ/J) \cdot (1/A) \quad (16)$$

and therefore,

$$A(N - N_0) = \ln(J/J_0) \quad (17)$$

where J₀ and N₀ correspond to the initial lower bound values of the J-integral and the number of cycles

below which the crack propagation law (Equation 11) does not hold.

The parameter A is assumed to be a material constant. To provide the appropriate condition for the assumption of parameter A, a loading condition should be set such that the size of the plastic zone ahead of the crack tip is constant and moving very slowly during propagation.

The upper limit of the validity of Equation 17 is when N tends toward N_{CY} and J tends toward J_{IC} ; hence,

$$c \rightarrow c_{\gamma} = J_{IC}/2Ue \quad (18)$$

Substituting into Equation 17 gives

$$A(N_{c\gamma} - N_0) = \ln J_{IC}/J_0 \quad (19)$$

where c_{CY} and N_{CY} are critical crack length and corresponding critical number of cycles at which the third phase of unstable failure commences.

Divide Equation 17 into Equation 19 to obtain

$$\ln(J/J_0)/\ln(J_1/J_0) = (N - N_0)/(N_c - N_0) = N/\Delta N_{c\gamma} \quad (20)$$

For Equation 20, J depends on assuming an initial detectable crack size in which a definition is required. The detectable length varies as a function of the measuring devices. Extremely short crack lengths are determined with extremely sensitive measuring devices like the scanning electron microscope and ultrasonic and acoustic emission. Alternatively, an "engineering size crack" that is detectable to the eye could be found experimentally as follows: N_0 to propagate different crack sizes should be recorded and a relationship between N_0/N_{CY} and c established. This relationship could be extrapolated to find the crack size c_0 at $N/N_{CY} = 0$.

From the c-J relationship, the value of c_0 is entered and the corresponding J_0 is obtained. This value should be substituted in Equation 20 instead of J_0 . Now Equation 20 will reduce to the nondimensional relationship,

$$J = f(\Delta N/\Delta N_f) \quad (21)$$

where N is the number of cycles required to propagate a crack from size c_0 to any arbitrary value c that corresponds to N.

Ultimate Failure Model

The ultimate failure model is defined by finding the number of cycles associated with unstable crack propagation. Unstable crack propagation occurs during the last cycles of fatigue life where the crack opens under extremely low loading conditions and, in this case, $J = J_{IC}$. The number of cycles from the critical crack size (c_{CY}) until complete failure is monitored experimentally for each initial crack size and denoted as ΔN_f .

A relationship between the dimensionless quantity c/D and ΔN_f , where D is the sample diameter, is established as a model for ultimate failure. The other alternative is to use the relationship between $\Delta c_f/D$ and ΔN_f , where Δc_f is the remaining length at the onset of unstable crack growth. The better correlated relationship will be used in this paper. In asphaltic mixtures, however, the contribution of this phase to fatigue life is minimal.

Matching Model

At this point, a form of relationship to serve as a matching criterion between notched and unnotched

specimen test results should be established to enable the determination of the number of cycles required to initiate an engineering size crack corresponding to c_0' . For this purpose, notched specimens should be subjected to the same stroke range loading conditions as the unnotched specimens, and the number of cycles required to initiate a detectable-to-the-eye crack recorded as N_0' . A regression line between N_0' from the notched specimens and N from the unnotched specimens will establish the required relationships.

Summary of the Proposed Fatigue Life Model

Fatigue life is then calculated according to the following formula:

$$N_f = N_0' + (\Delta N_{c\gamma}) + (\Delta N_f) \quad (22)$$

where

- N_f = total fatigue life.
- N_0' = number of cycles to initiate a crack, c_0' ; this is obtained (at present) from the matching model.
- $(\Delta N_{c\gamma})$ = number of cycles required to propagate a crack from c_0' to c_{CY} ; this is obtained from the crack propagation model.
- (ΔN_f) = number of cycles required to open the crack from c_C to ultimate failure; this is obtained from the ultimate failure model.

The simple procedure for determining these terms is as follows:

1. Establish cyclic plasticity fatigue curve using σ_f , E, and C_f from routine monotonic tests and the universal slopes b and c established in this paper.
2. Run fatigue tests on notched discs together with J-integral testing.
3. Use Equation 19 to obtain $(\Delta N_{c\gamma})$.
4. For any selected N_f value from Step 1, enter the matching model to get N_0 .
5. Use the ultimate failure model to obtain (ΔN_f) .
6. Add to get the total fatigue life as in Equation 22.

EXPERIMENTATION

Marshall-type specimens were prepared from a laid recycled mix (20) and processed for determination of parameters in the developed models. Samples for the controlled stroke fatigue testing were unnotched Marshall-type specimens prepared according to ASTM D1559. Samples for the J-integral and fatigue crack propagation models were notched Marshall-type specimens with various initial crack lengths. The notches were made by sawing the specimens to a depth of 0.75 in. Cracks were created by applying static loads.

Controlled Stroke Testing

Samples were subjected to a controlled stroke amplitude (U) ranging from 5×10^{-4} to 186×10^{-4} in. at a frequency of 60 cpm. Test results are given in Table 1. The relationship between the total strain range ($\Delta \epsilon$) and the number of cycles to failure (N_f) is plotted on a semilog scale (Figure 2), the strain being on the arithmetic scale and the N_f being on the logarithmic scale. Tangents were drawn at both

TABLE 1 Fatigue on Discs

Stroke Control Test No. ^a	Stroke Δu (in.)	$\Delta \epsilon$ (%) $\times 10^{-1}$	N_f
1	0.0005	0.125	11,789
2	0.0024	0.6	9,894
3	0.0048	1.2	1,964
4	0.0076	1.9	1,224
5	0.186	4.65	150

Note: Frequency = 60 cpm; sample: $t = 2\frac{1}{2}$ in., $D = 4.00$ in.

^aAverage of three samples per test.

sides of this curve and their slopes and intercepts with the strain range scale were found to be

$$\Delta \epsilon_E = 1.9 * 10^{-1} \% \text{ at } N_f = 1; \text{ slope} = -0.0422 \tag{23}$$

$$\Delta \epsilon_\rho = 12.9 * 10^{-1} \% \text{ at } N_f = 1; \text{ slope} = 0.387 \tag{24}$$

where $\Delta \epsilon_E$ is the intercept of the fatigue strength line and $\Delta \epsilon_\rho$ is the intercept of the fatigue ductility line.

Hence,

$$\Delta \epsilon_E = 0.2094 N_f^{-0.0422} \tag{25}$$

$$\Delta \epsilon_\rho = 3.1445 N_f^{-0.387} \tag{26}$$

Then the total strain is related to the number of cycles to failure by

$$\Delta \epsilon = \Delta \epsilon_E + \Delta \epsilon_\rho = 0.2094 N_f^{-0.0422} + 3.1445 N_f^{-0.387} \tag{27}$$

Comparing the coefficients of this equation with those of Equation 7 reveals

$$\sigma_f' = 0.2094$$

and

$$A_2' \times D' = 3.1445$$

but

$$D' = 1.29\%$$

Therefore

$$A_2' = 2.437$$

Hence, Equation 27 can be written as

$$\Delta \epsilon = A_1 (\sigma_f/E) N_f^{-0.0422} + 2.437 A_2 D N_f^{-0.387} \tag{28}$$

where

- $A_1 = \sigma_f' / \sigma_f =$ fatigue dynamic stress ratio;
- $A_2 = D' / D =$ fatigue dynamic ductility ratio;
- $\sigma_f, D =$ monotonic fracture strength and ductility, respectively; and
- $\sigma_f, D' =$ corresponding values of σ_f and D as extrapolated to $N_f = 1$ in the controlled stroke fatigue testing.

The fatigue dynamic ratios (A_1 and A_2) need to be found statistically. Because of the limited amount of available data, these coefficients are determined here with values to serve as an illustration. However, by assumption (21), $A_1 = A_2 = 1$. Furthermore, indirect tensile strength tests were carried out on six samples and the deformation was recorded. Results of these tests were

$$\sigma_f = 41.1 \pm 3 \text{ psi and } D\% = 1.28 \pm 0.04 \text{ (average values)}$$

But

$$\begin{aligned} \sigma_f' &= E \times 0.2094 \times 10^{-3} \\ &= 0.215 \times 10^6 \times 0.2094 \times 10^{-3} = 45 \text{ psi} \\ D &= 1.29\% \end{aligned}$$

and

$$D' = 1.29\% \text{ (from Figure 2).}$$

Therefore,

$$A_1 = 1.09, A_2 = 1.0078 \cong 1$$

and hence the controlled stroke fatigue curve can be constructed from the following relationship:

$$\epsilon = 1.095 (\sigma_f/E) N_f^{-0.0422} + 2.437 D N_f^{-0.387} \tag{29}$$

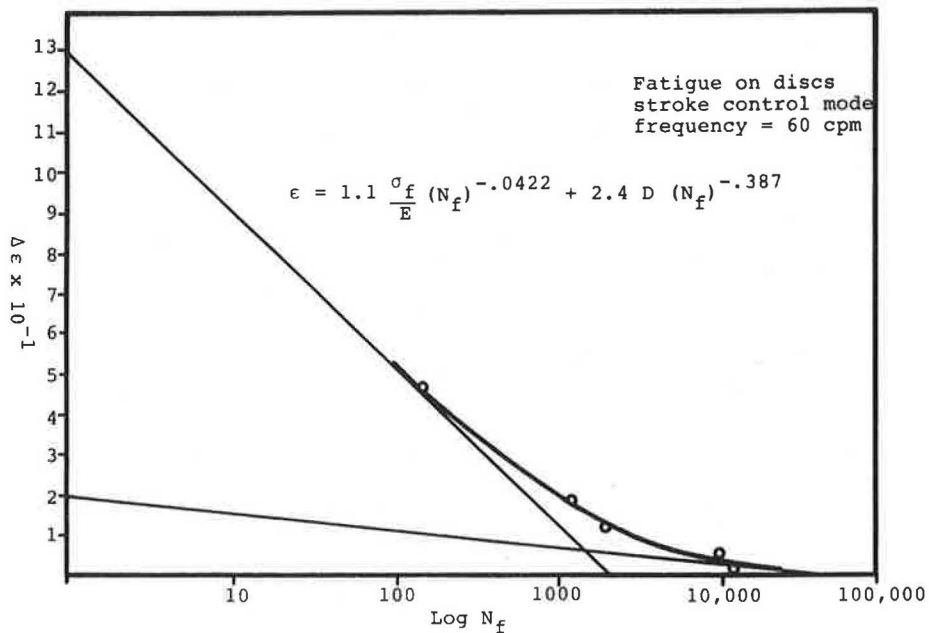


FIGURE 2 Controlled stroke fatigue on unnotched discs.

where σ_f , D, and E are to be found experimentally from any monotonic testing program.

Matching Model

Notched specimens were subjected to the same stroke range as was used in the fatigue testing. The number of cycles to initiate a crack was recorded and the crack was monitored to failure (Table 2). The results at high stroke range were extrapolated from low stroke range test results. The number of cycles to initiate a crack was plotted against the number of cycles to failure for the corresponding stroke ranges. The relationship was found by linear regression as follows:

$$\log N_f = 1.86537909 + 0.79051038 \log (N) \quad (30)$$

$$R^2 = 0.963584$$

J-Integral Testing

Notched Marshall-type samples with different initial crack sizes were tested in a load control mode with rate of loading = 1,000 psi per minute. The load (P) versus displacement (δ) curve test results are given in Table 3 and were plotted on an arithmetic scale paper. The areas under the P- δ curves were found at displacements of 2, 4, 6, 8, and 10 in. $\times 10^{-2}$ and are given in Table 4. This table is used

to find the relationship U/B versus c_0 , which is plotted on arithmetic scale paper. The slope of the curves between U/B and c_0 is the J-integral value, which was found at the different initial crack sizes and plotted in Figure 3 as J-integral versus δ . It is noted from Figure 3 that J_{IC} can be found directly at the points of crack starting to open (i.e., displacement under no change in J-values). This was checked against actual monitored displacement under incipient crack conditions. It is of interest to compare values of the J_{IC} and elastic fracture toughness (K_{IC}) because J-integral testing included the K_{IC} testing method. Table 5 gives the results, with the last column indicating the corresponding values of E.

Fatigue Crack Propagation Model Verification

Notched Marshall-type specimens with different initial crack sizes were tested in load control mode. The test setup was the same as that used in K_{IC} testing. The number of cycles to propagate the crack was recorded, and the number of cycles to advance the crack each 0.5 cm thereafter was monitored. Test results are given in Table 6. The crack (c) versus number of cycles (N) relationship was fitted using nonlinear least squares approximation. The general form of the fitted equation thus obtained is

$$c = c_0 A N^n \quad (31)$$

TABLE 2 Matching Model Test Results

Sample No : L2% Mix No. 6		Stroke = 0.2 (in * 10 ⁻³)			C ₀ = 0.0			
Crack Length (cm)	North crack (cm)	0+	0.5	1.0	1.5	2.0	2.5	3.0
	South crack (cm)	0+	0.51	1.0	1.5	2.0	2.5	3.0
No. of Cycle	N (cycles*10 ²)	2090	2440	2865	3145	3260	3.0	3337

Sample No : L2% Mix No. 6		Stroke = 0.2 (in * 10 ⁻³)			C ₀ = 0.0			
Crack Length (cm)	North crack (cm)	3.5	4.0	4.5				Failure
	South crack (cm)	3.5	4.0	4.5				
No. of Cycle	N (cycles*10 ²)	3395	3358	3363				3374

Sample No : L5% Mix No. 6		Stroke = 0.5 (in * 10 ⁻³)			C ₀ = 0.0			
Crack Length (cm)	North crack (cm)	0+	0.5	1.0	1.5	2.0	2.5	3.0
	South crack (cm)	0+	0.7	2.0	3.0	3.5	3.7	3.0
No. of Cycle	N (cycles*10 ²)	2080	2444	2740	2900	3130	3150	3165

Sample No : L5% Mix No. 6		Stroke = 0.5 (in * 10 ⁻³)			C ₀ = 0.0			
Crack Length (cm)	North crack (cm)	3.5	4.0	4.5				Failure
	South crack (cm)	4.1	4.5	4.5				
No. of Cycle	N (cycles*10 ²)	3172	3190	3200				3275

TABLE 2 continued

Mode of loading : Stroke Control.

Sample NO: L10% Mix NO: 6		Stroke = 2.4 (in * 10 ⁻³)					C ₀ = 0.0	
Crack Length (cm)	North crack (cm)	0 ⁺	0.5	1.0	1.5	2.0	2.5	3.0
	South crack (cm)	0 ⁺	0.7	1.3	2.0	2.6	2.9	3.3
No. of Cycle	N (cycles*10 ²)	105	140	176	187	195	204	215

Sample No: L8% Mix No. 6		Stroke = 2.0 (in * 10 ⁻³)					C ₀ = 0.0	
Crack Length (cm)	North crack (cm)	0 ⁺	0.5	1.0	1.5	2.0	2.5	3.0
	South crack (cm)	0 ⁺	0.3	2.0	2.0	2.5	2.7	3.0
No. of Cycle	N (cycles*10 ²)	157	346	800	889	930	990	1160

Sample No : L8% Mix No. 6		Stroke = 2.0 (in * 10 ⁻³)					C ₀ = 0.0	
Crack Length (cm)	North crack (cm)	3.5	4.0	4.5				Failure
	South crack (cm)	3.5	4.0	4.5				
No. of Cycle	N (cycles*10 ²)	1228	1236	1250				1268

Sample No : L12% Mix No. 6		Stroke = 3.6 (in * 10 ⁻³)					C ₀ = 0.0	
Crack Length (cm)	North crack (cm)	0 ⁺	0.5	1.0	1.5	2.0		Failure
	South crack (cm)	0 ⁺	0.7	1.5	1.9	2.4		
No. of Cycle	N (cycles*10 ²)	275	287	295	300	304		319

TABLE 3 p-δ Results

Sample No.	C ₀ (in.)	Load and Displacement (lb and in. x 10 ⁻²)											
LM-4	0.25												
	Load	0	150	350	625	900	1,100	1,225	1,200	975	750		
	Displacement	0	1.25	2.5	3.75	4.38	5.63	6.25	7.5	8.75	10.0		
LM-5	0.25												
	Load	0	25	237.5	500	1,075	1,187.5	1,325	1,325	1,025	600	412.5	
	Displacement	0	0.625	1.25	2.5	3.75	4.38	5.63	6.88	7.5	8.75	10	
LM-10	0.5												
	Load	0	37.5	262.5	575	900	1,125	1,225	1,125	887.5	675	512.5	
	Displacement	0	0.63	1.88	2.5	3.75	5.0	5.63	6.88	8.13	8.75	10	
LM-11	0.5												
	Load	0	50	375	825	1,225	1,350	1,350	1,350	950	575	487.5	
	Displacement	0	0.63	1.88	2.5	3.75	5.0	6.25	6.88	8.13	8.75	10	
LM-13	0.75												
	Load	0	25	137.5	375	650	900	1,025	1,000	825	650	500	
	Displacement	0	1.88	2.5	3.75	5.0	5.63	6.88	8.13	8.75	10.0	11.25	
LM-15	0.75												
	Load	0	25	100	250	450	650	825	912.5	900	762.5	575	
	Displacement	0	1.88	2.5	3.75	5.0	5.63	6.88	8.13	8.97	10.0	11.25	
LM-21	1.00												
	Load	0	25	100	250	450	700	900	975	875	650	462.5	
	Displacement	0	1.88	3.13	4.38	5	6.25	7.5	8.75	9.38	10.63	11.25	
LM-26	1.00												
	Load	0	87.5	212.5	450	725	1,000	1,150	1,125	825	550		
	Displacement	0	1.25	2.5	3.75	4.38	5.63	6.25	7.5	8.75	10.0		
LM-31	1.25												
	Load	0	62.5	175	400	600	700	650	512.5	375	275		
	Displacement	0	1.25	1.88	3.13	4.38	5.0	6.25	7.5	8.13	9.38		
LM-32	1.25												
	Load	0	125	325	437.5	550	600	550	437.5	337.5	275		
	Displacement	0	1.25	2.5	3.13	4.38	5.63	6.88	7.5	8.75	10.0		

where

- c = crack length,
- c₀ = initial crack length,
- N = number of cycles at crack length c, and
- A, n = constants to be found experimentally.

Nonlinear least squares fitting of the c-N data is plotted in Figure 4. The mathematical expressions for these relationships are

- For c₀ = 0.25 in., c/c₀ = 3.5502662 x 10⁻² NE^{2.895} with R² = 0.96
- For c₀ = 0.50 in., c/c₀ = 1.1889786 x 10⁻⁷ NE^{1.847} with R² = 0.977
- For c₀ = 0.75 in., c/c₀ = 1.5500153 x 10⁻⁹ NE^{2.41} with R² = 0.985
- For c₀ = 1.0 in., c/c₀ = 4.965967 x 10⁻³ NE^{3.679} with R² = 0.969
- For c₀ = 1.5 in., c/c₀ = 2.2545445 x 10⁻¹⁷ NE^{4.936} with R² = 0.987

Development of the Relationship dc/dN Versus J with Worked Example

The development of this relationship will be illustrated by an example using c₀ = 0.5 in.

1. The relationship dc/dN is found as a function of N. For c = 0.5 in., the relationship is

$$dc/dN = 1.0980217 \times 10^{-7} N \text{ in./cycle}^{0.847} \tag{32}$$

2. Table 7 is constructed using the relationship obtained in Step 1.
3. From the graphs of P-δ, the relationship

TABLE 4 U/B Values

c ₀ (in.)	δ in. x 10 ⁻²				
	2	4	6	8	10
0.25	320	1,840	4,380	6,830	8,230
0.5	232	1,692	4,222	6,682	8,072
0.75	0.0	450	1,680	3,600	5,340
1.00	14	574	1,984	3,984	5,704
1.25	131	901	2,151	3,181	5,131

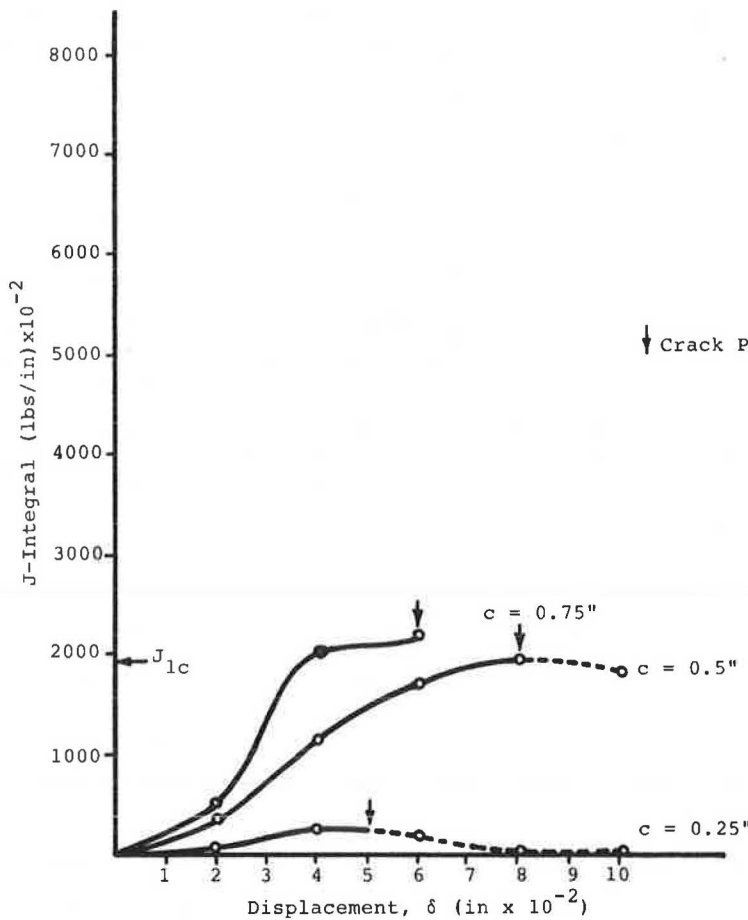


FIGURE 3 J-integral versus displacement for different initial crack lengths.

TABLE 5 K_{1c} - J_{1c} Comparison

c ₀	Thickness t (in.)	P _{fail} (lb)	K _{1c} ^a (psi)	J _{1c} (lb/in. x 10 ⁻²)	E = (K _{1c} ² /J _{1c}) x [1/(1 - μ ²)] (psi)
0.25	2.6	1,287.5	496.9		
0.5	2.60	1,225	531	1,900	169.2 x 10 ²
0.75	2.55	987.5	540	1,900	174.9 x 10 ²

^aK = F_{stress} x F_{geom} c (P/tR) where F_{stress} = 6.53078 e^{4.30577} (c/R)^{2.475}, F_{geom} = 3.950373 e^{-3.07103} (c/R)^{0.25}, R = radius, t = thickness, P = vertical applied load, and μ = 0.35.

TABLE 6 c-N Test Results at P = 200 lb

C ₀ (in.)	N (cm)										Failure	
	0+	0.5	1.0	1.5	2.00	2.5	3.00	3.5	4.00	4.50		5.0
0.25	2900	8100	12 300	12 600	12 700	12 900	15 300	16 900	17 160	17 500	17 640 ^b	17 650
0.5	2300	3775	4270	6070	7320	8500	9820	9580	10 105	10 210 ^b		10 230
0.75	1500	2510	3450	4300	4800	5400	5600	5800	5880 ^b			5913
1.0	1170	2100	2450	2750	3225	3485 ^b	3530					3550
1.5	650	1580	1750	1960	2115	2210 ^b	2240					2242
0.75 ^a	450	735	850	1000	1030 ^b	1037	1039	1040			1047	1042

^aP = 300 lb. ^bUnstable crack propagation.

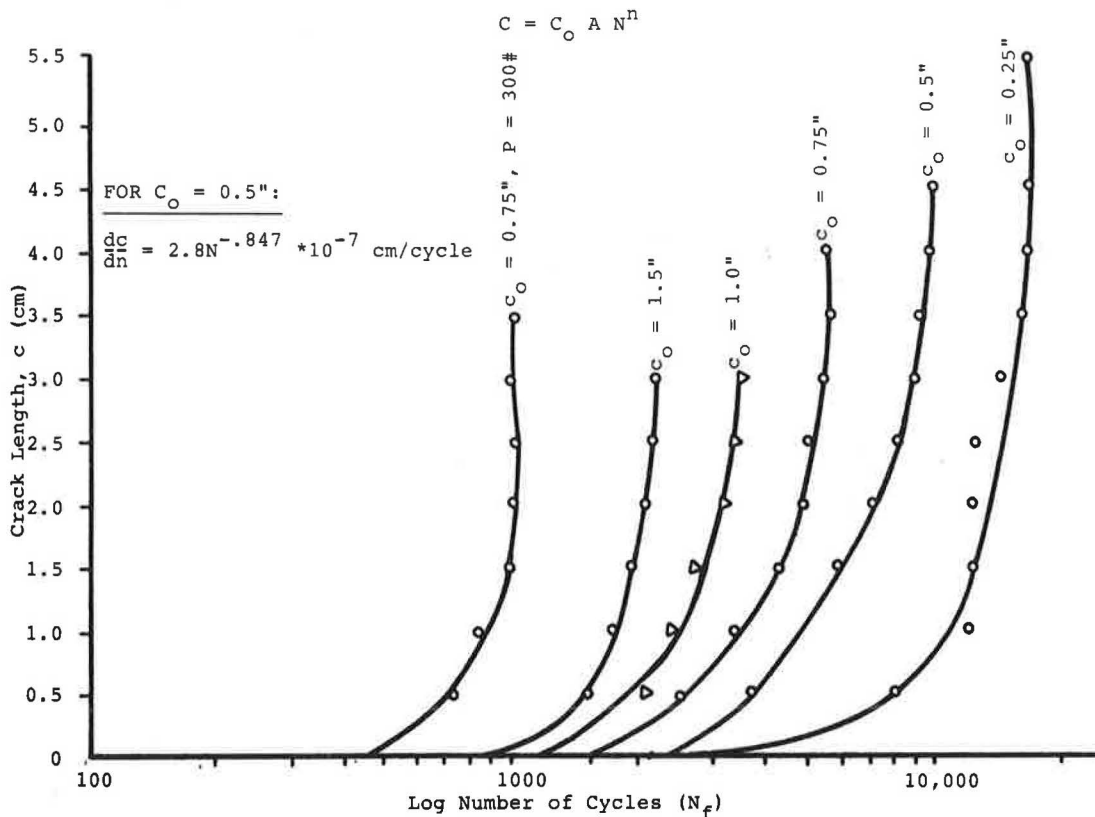


FIGURE 4 C-N relationship.

TABLE 7 Worked Example for C₀-0.5 in.

	N					
	3,000	4,000	5,000	6,000	7,000	10,000
c x 10 ⁻⁵	1.57	2.67	4.04	5.65	7.52	14.53
dc/dN x 10 ⁻²	9.677	12.35	14.92	17.41	19.83	26.83
J x 10 ⁻²	-	100	200	250	650	1,900

c-δ can be constructed for the same loading amplitude used to develop the C-N relationship. This gives the corresponding fourth row in Table 7.

4. For those values of δ, values of J-integral are found in Figure 3. These values are given in the fifth row of Table 7.

5. The relationship dc/dN is now ready to be fitted with J-integral values. The fitted relationship is shown in Figure 5, and has the form

$$dc/dN \begin{cases} 10000 + 28.57 J * 10^{-8} \text{ in./cycle} \dots 10^{-6} < dc/dN < 1.8 * 10^{-6} \\ 17000 + 4.865 J * 10^{-8} \text{ in./cycle} \dots 1.8 * 10^{-6} < dc/dN < 2.6 * 10^{-5} \\ J_{IC} * 10^{-5} \text{ in./cycle} \dots \text{for } dc/dN > 2.6 * 10^{-6} \end{cases} \quad (33)$$

Ultimate Failure Model

A linear regression relationship was fitted between ΔN_f versus c/D and ΔN versus c_f/D. These relationships were found to be

$$\Delta N_f = 22.01408451 + 11.26760563 \Delta c_f/D \quad R^2 = 0.868 \quad (34)$$

$$\log \Delta N_f = 2.05451064 + 0.82823077 \log c/D \quad R^2 = 0.883 \quad (35)$$

CONCLUSIONS

1. A simple procedure for constructing the stroke control fatigue curve was illustrated and is based on simple routine laboratory tests compiled with the universal slopes b and c established in this work. The fatigue life analysis is then based on monotonic material strength and ductility parameters. This approach will help highway engineers acquire greater experience with pavement life evaluation.

2. A J-integral test method for asphaltic mixtures was established. This method includes the test method for K_{IC}. The value of the J_{IC} fracture tough-

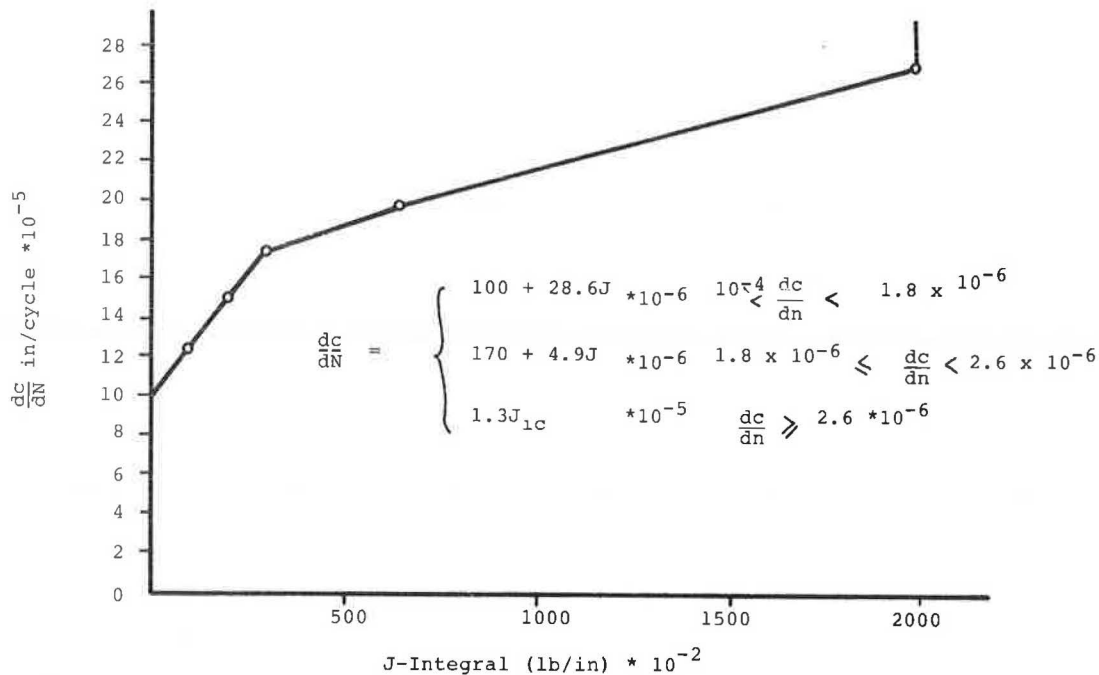


FIGURE 5 dc/dN versus J-integral relationship.

ness is compared to that of K_{IC} showing that, although differences exist between the two, a trend relationship probably exists. More experimentation is needed if a relationship is to be found.

3. A crack propagation model showed a linear relationship between dc/dN and J . This model is recommended for use in the fatigue life analysis of flexible pavements instead of that of dc/dN versus K because it only requires an experimentation phase and accounts for both elastic and plastic fracture behavior.

4. A crack initiation model and ultimate failure model were established. The general method of finding fatigue life using elasto-plastic fracture mechanics was illustrated.

REFERENCES

1. C.F. Rogers et al. Nationwide Survey of Pavement Terminal Serviceability. In HRB Record 42, HRB, National Research Council, Washington, D.C., 1963, pp. 26-44.
2. Revision of Section II, Manual on Fatigue Testing. Special Technical Publication 91, ASTM, Philadelphia, Pa., 1959.
3. F. Moavenzadeh, J.R. Soussou, and H.K. Findakly. A Stochastic Model for Prediction of Accumulative Damage in Highway Pavements. Massachusetts Institute of Technology, Cambridge, 1971.
4. T.M.H. Von Karman. Forschungsarbeiten Deutscher Ingenieur, Pt. 118, 1912, pp. 37-68.
5. B. Mukberejee and D.J. Burne. Growth of Part Through Thickness Fatigue Cracks in Sheet Polymethylmethacrylate. Engineering Fracture Mechanics, Vol. 4, No. 4, 1972.
6. C. Monismith and J.A. Deacon. Fatigue of Asphalt Paving Mixtures. Journal of the Transportation Engineering Division, ASTM, No. TE2, 1969.
7. P. Basin et al. Deformability, Fatigue and Healing Properties of Asphalt Mixes. Proc., Second International Conference on Structural Design of Asphalt Pavements, Ann Arbor, Mich., 1967.
8. B. Coffman. The Fatigue of Flexible Pavements. Final Report EES 296-B-1. Ohio State University Engineering Experiment Station, Columbus, 1971.
9. Savin. Stress Concentration Around Holes. Pergamon Press, New York, 1966.
10. C.L. Monismith. Viscoelastic Behavior of Asphalt Concrete Pavements. Proc., International Conference on Structural Design of Asphalt Pavements, 1963.
11. J.A. Deacon and C.L. Monismith. Laboratory Flexural-Fatigue Testing of Asphalt-Concrete with Emphasis on Compound-Loading Tests. In HRB Record 158, HRB, National Research Council, Washington, D.C., 1967, pp. 1-31.
12. P.S. Pell. Fatigue of Asphalt Pavement Mixes. Proc., Second International Conference on Structural Design of Asphalt Pavements, Ann Arbor, Mich., 1967.
13. K. Majidzadeh et al. Development and Field Verification of a Mechanistic Structural Design System in Ohio. Proc., 4th International Conference on Structural Design of Asphalt Pavements, Ann Arbor, Mich., 1977.
14. K. Majidzadeh et al. Application of Fracture Mechanics for Improved Design of Bituminous Concrete. Final Report RF3736. Ohio State University Research Foundation, Columbus, 1967.
15. G.P. Cherepanov. On the Theory of Fatigue Crack Growth. Engineering Fracture Mechanics, Vol. 4, 1972.
16. S.S. Manson. Interfaces Between Fatigue, Creep and Fracture. International Journal of Fracture Mechanics, Vol. 1-2, 1965-1966, pp. 327-363.
17. J. Morrow. Cyclic Plastic Strain Energy and Fatigue of Metals. In Special Technical Publication 378: Internal Friction, Damping and Cyclic Plasticity, ASTM, Philadelphia, Pa., 1965, pp. 45-87.
18. W. Weibull. Fatigue Testing and Analysis of Results. Pergamon Press, New York, 1960.

19. J.A. Begeley and J.D. Landes. Special Technical Publication 514. ASTM, Philadelphia, Pa., 1972, pp. 1-20.
20. A.A. Abdulshafi. Viscoelastic/Plastic Characterization Rutting and Fatigue of Flexible Pavements. Ph.D. dissertation. Ohio State University, Columbus, 1983.
21. G.R. Halford and J. Morrow. Low Cycle Fatigue in Torsion. Proc., ASTM, Philadelphia, Pa., Vol. 62, 1962.

Publication of this paper sponsored by Committee on Characteristics of Bituminous Paving Mixtures to Meet Structural Requirements.

Importance and Cost-Effectiveness of Testing Procedures Related to Flexible Highway Pavement Construction in Florida

JOHN M. LYBAS, BYRON E. RUTH, and KARL W. KOKOMOOR

ABSTRACT

The cost-effectiveness of in-place density testing procedures for flexible highway pavement construction in Florida was determined using statistical analyses of test results from typical construction projects. The analyses were performed to establish the probability of density test failure, and corresponding margin of failure, for different levels of testing and lengths of projects. Materials analyzed included embankment, stabilized subgrade, limerock base, and asphalt concrete pavement. A reduction in apparent structural strength due to density test failure was computed on the basis of relationships established between elastic moduli and density. This structural deficiency was corrected by an additional thickness of material sufficient to reduce the pavement surface deflection to the same level as that encountered in a properly constructed pavement. An elastic layer computer program was used to determine these additional thicknesses. The cost-effectiveness of any particular testing frequency was based on the cost of testing plus the cost of the additional material to correct for deficient density. Results indicated that current density testing frequencies are generally cost-effective for projects 3 or more miles in length, with the exception of the limerock base, for projects barely 3 mi long, where increased testing was indicated, and for projects 10 or more miles in length, where reduced testing frequencies could be considered. For projects 1 mi long and shorter, for embankment, stabilized subgrade, and limerock base, results indicated that testing frequencies needed to be increased to attain cost-effectiveness.

Test methods for the control and acceptance of flexible pavement construction have evolved over the years. The Florida Department of Transportation (FDOT) "Sampling and Testing Guide" and current specifications are periodically revised to incorporate improvements derived from research and changes in technology. Statistically based quality assurance specifications are currently in use for asphalt concrete pavement construction.

Although the testing requirements and specifications are considered reliable, the FDOT was concerned about the cost-effectiveness of the testing program and wanted to ascertain if testing frequency could be altered to provide cost savings without a

reduction in quality. This question was addressed in a research program that encompassed a review of current testing procedures for highway pavements, the determination of the costs of testing, the collection of test results from several highway projects, and a statistical analysis to determine how altering the frequency of testing would affect cost.

OVERVIEW

Although a number of material tests were included in the FDOT study, the major emphasis was on density tests for asphalt and underlying foundation mate-